Metabolism Is Required for the Expression of Ecstasy-Induced Cardiotoxicity in Vitro

Márcia Carvalho,*,† Fernando Remião,† Nuno Milhazes,‡,§ Fernanda Borges,‡ Eduarda Fernandes,† Maria do Céu Monteiro,§ Maria José Gonçalves,§ Vítor Seabra,§ Francisco Amado,|| Félix Carvalho,† and Maria Lourdes Bastos†

REQUIMTE, Serviço de Toxicologia and Serviço de Química Orgânica, Faculdade de Farmácia, Universidade do Porto, Rua Aníbal Cunha, 164, 4099/030 Porto, Portugal, Instituto Politécnico de Saúde-Norte, R. Central da Gandra, 1317, Gandra, 4585/116 Paredes, Portugal, and Departamento de Química, Universidade de Aveiro, 3810/123 Aveiro, Portugal

Received January 23, 2004

Cardiovascular complications associated with 3,4-methylenedioxymethamphetamine (MDMA, ecstasy) abuse have increasingly been reported. The indirect effect of MDMA mediated by a sustained high level of circulating biogenic amines may contribute to the cardiotoxic effects, but other factors, like the direct toxic effects of MDMA and its metabolites in cardiac cells, remain to be investigated. Thus, the objective of the present in vitro study was to evaluate the potential cardiotoxic effects of MDMA and its major metabolites 3,4-methylenedioxyamphetamine (MDA), N-methyl-α-methyldopamine (N-Me-α-MeDA), and α-methyldopamine (α-MeDA) using freshly isolated adult rat cardiomyocytes. The cell suspensions were incubated with these compounds in the final concentrations of 0.1, 0.2, 0.4, 0.8, and 1.6 mM for 4 h. α-MeDA, N-Me-α-MeDA, and their respective aminochromes (oxidation products) were quantified in cell suspensions by HPLC-DAD. The toxic effects were evaluated at hourly intervals for 4 h by measuring the percentage of cells with normal morphology, glutathione (GSH), and glutathione disulfide (GSSG); intracellular Ca^{2+}, ATP, and ADP; and the cellular activities of glutathione peroxidase, glutathione reductase, and glutathione-S-transferase. No toxic effects were found after exposure of rat cardiomyocytes to MDMA or MDA at any of the tested concentrations for 4 h. In contrast, their catechol metabolites N-Me-α-MeDA and α-MeDA induced significant toxicity in rat cardiomyocytes. The toxic effects were characterized by a loss of normal cell morphology, which was preceded by a loss of GSH homeostasis due to conjugation of GSH with N-Me-α-MeDA and α-MeDA, sustained increase of intracellular Ca^{2+} levels, ATP depletion, and decreases in the antioxidant enzyme activities. The oxidation of N-Me-α-MeDA and α-MeDA into the toxic compounds N-methyl-α-methyldopaminochrome and α-methyldopaminochrome, respectively, was also verified in cell suspensions incubated with these MDMA metabolites. The results obtained in this study provide evidence that the metabolism of MDMA into N-Me-α-MeDA and α-MeDA is required for the expression of MDMA-induced cardiotoxicity in vitro, being N-Me-α-MeDA the most toxic of the studied metabolites.

Introduction

MDMA[1] (ecstasy) is an amphetamine derivative, which has become increasingly popular as a recreational drug of abuse mainly among young people. MDMA consumption has been recently related to several reports of cardiovascular toxicity (*1*−*3*). Indeed, an acute administration of MDMA increases heart rate, blood pressure, and myocardial oxygen consumption in both humans (*4*, *5*) and animals (*6*), which may ultimately result in tachycardia, hypertension, arrhythmias, cardiac ischemia, and heart failure. The chronic use of MDMA may also result in serious cardiovascular damage. A daily administration of MDMA to rats for a total of 28 days was reported to produce significant myocardial pathologies including contraction band necrosis, inflammation, fibrosis, and ultrastructural changes (*7*). These findings are in agreement with a previous report of similar heart pathological alterations in five victims of MDMA use (*2*).

Although there is undeniable evidence of MDMA-induced cardiac toxicity, the mechanism(s) responsible for that toxicity remain to be clarified. One proposed mechanism suggests that the sustained increased catecholaminergic stimulation, a consequence of MDMA intake, is responsible for the MDMA cardiotoxicity. Indeed, the abnormal high release of monoamines from peripheral sympathetic nerves in cardiovascular tissues was reported to produce myocardial necrosis (*8*, *9*). In addition, behavioral and environmental factors accompanying illicit MDMA use may increase the risk for cardiovascular complications. MDMA consumption in crowded conditions, high ambient temperature, loud

* To whom correspondence should be addressed. Fax: 351-222003977. E-mail: marciacarvalho@ff.up.pt.
† Serviço de Toxicologia, Universidade do Porto.
‡ Serviço de Química Orgânica, Universidade do Porto.
§ Instituto Politécnico de Saúde-Norte.
|| Universidade de Aveiro.

[1] Abbreviations: MDMA, 3,4-methylenedioxymethamphetamine; MDA, 3,4-methylenedioxyamphetamine; N-Me-α-MeDA, N-methyl-α-methyldopamine; α-MeDA, α-methyldopamine; GPX, selenium-dependent glutathione peroxidase; GR, glutathione reductase; GST, glutathione-S-transferase; ROS, reactive oxygen species; RNS, reactive nitrogen species; H_2O_2, hydrogen peroxide; Fluo-3 AM, fluo-3-acetoxymethyl ester; PI, propidium iodide; DAD, diode array detection.

10.1021/tx049960f CCC: $27.50
Published on Web 04/27/2004

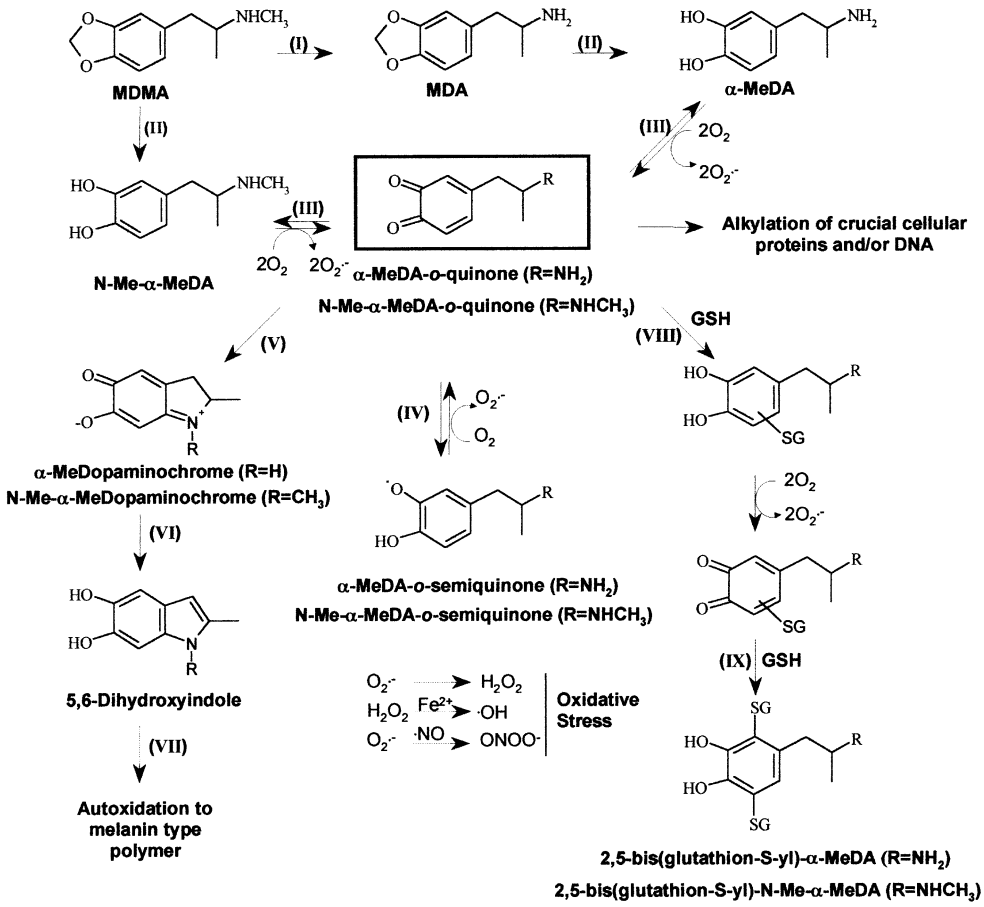

Figure 1. Proposed pathway for MDMA metabolism into cardiotoxic metabolites. MDMA can undergo N-demethylation to MDA (**I**). Cytochrome P450 mediates demethylenation of MDMA and MDA to N-Me-α-MeDA and α-MeDA, respectively (**II**). The catechols are readily oxidized to the corresponding *ortho*-quinones (**III**), which can enter redox cycles with their semiquinone radicals, leading to formation of ROS (**IV**). On cyclization, *ortho*-quinones give rise to the formation of aminochromes (**V**) and related compounds, such as 5,6-dihydroxyindoles (**VI**), which can undergo further oxidation and polymerization to form brown or black insoluble pigments of melanin type (**VII**). Alternatively, *ortho*-quinones can react readily with GSH to form the corresponding GSH conjugates (**VIII**, **IX**).

noise places, and intense physical activity (as frequently occurs at "rave parties") may be associated with a potential life-threatening increase in the cardiovascular toxicity of MDMA. In line with this, Gesi et al. (*10*) recently reported that concomitant exposure to MDMA and noise in rats produced changes in the heart ultrastructure, particularly evident at the mitochondrial level, namely, disarranged cristae and a less dense matrix. An alternative mechanism for MDMA-induced myocyte damage may be a direct toxic effect of MDMA or its metabolites in cardiac cells. It was already reported that methamphetamine is toxic to myocytes in culture systems devoid of catecholamines (*11*). In addition, MDMA metabolism results in the formation of redox active metabolites, which have recently been implicated in the mechanisms underlying ecstasy-induced neurotoxicity (*12*−*15*), hepatotoxicity (*16*), and nephrotoxicity (*17*).

Metabolism of MDMA involves N-demethylation to MDA. MDMA and MDA are O-demethylenated to N-Me-α-MeDA and α-MeDA, respectively (*18*−*20*), both of which are catechols that can undergo oxidation to the corresponding *ortho*-quinones (Figure 1). Quinones are highly redox active molecules that can undergo redox cycling, which originates semiquinone radicals and leads to the generation of ROS or RNS (*21*). Quinones can also be oxidized, in a process that involves an irreversible 1,4-intramolecular cyclization reaction, resulting in the formation of aminochromes (colored pigments) and related compounds, such as 5,6-dihydroxyindoles, which eventually leads to the appearance of brown or black insoluble polymers of the melanin type (*22*, *23*). The catecholamine oxidation process can be catalyzed under physiological conditions by oxidative enzymes, such as xanthine oxidase, peroxidase, lipoxygenase, several copper-containing catechol oxidases, or in the presence of metal ions such as Cu^{2+}, Mn^{2+}, Fe^{3+}, and several copper and ferric chelates (*23*). Alternatively, as the reactive *o*-quinone intermediates are Michael acceptors, cellular damage can occur through alkylation of crucial cellular proteins and/or DNA. In the presence of GSH, *o*-quinone may be conjugated with GSH to form a glutathionyl adduct (*24*). This GSH conjugate remains redox active being readily oxidized to the quinone-thioether, which, after the reductive addition of a second molecule of GSH, yields a 2,5-bis-glutathionyl conjugate (*15*). Taken all together, MDMA metabolism leading to the formation of ROS and/or toxic oxidation products and/or GSH depletion may represent the triggering factor responsible for the cardiotoxicity exerted by this amphetamine.

In view of the scarce data regarding the mechanism(s) underlying MDMA-induced toxicity on the cardiovascular system, the purpose of this study was to investigate the role of metabolites in MDMA-induced cardiotoxicity.

Materials and Methods

Chemicals. Collagenase (type II) was obtained from Worthington (U.S.A.). Fluo-3 AM and PI were obtained from Molecular Probes (Eugene, OR). All other reagents used in this study were of analytical grade. MDMA (HCl salt), MDA (HCl salt), N-Me-α-MeDA (HCl salt), and α-MeDA (HBr salt) were synthesized in the Organic Chemistry Department, Porto University (Portugal).

Cardiomyocyte Isolation and Incubation. Cardiomyocytes were isolated by collagenase and protease perfusion as previously described (*25*). Adult male Wistar rats (Charles-River Laboratories, Barcelona, Spain), weighing 200−250 g, were used. Cell viability at the beginning of the experiments was 70 ± 5%.

Incubations were performed in a water bath at 37 °C, using 2.5×10^5 cells/mL in modified Krebs−Henseleit buffer supplemented with 1.8 mM $CaCl_2$ (pH 7.2) and saturated with an airstream of carbogen. Isolated cardiomyocytes were preincubated for 30 min at 37 °C and then incubated with MDMA, MDA, N-Me-α-MeDA, or α-MeDA at a final concentration of 0.1, 0.2, 0.4, 0.8, or 1.6 mM for 4 h. Because α-MeDA and N-Me-α-MeDA are light sensitive unstable compounds, all incubations were performed with light protection. Cell suspension aliquots taken at time 0 and at hourly intervals for 4 h were used for the evaluation of cell morphology, ATP and ADP levels, and concentrations of α-MeDA, N-Me-α-MeDA, and their respective aminochromes (for the last parameter, quantifications were only performed in cell suspensions incubated with the highest concentration assayed). GSH and glutathione disulfide (GSSG) were measured in aliquots taken at time 0 and each hour during 2 h of incubation. GPX, GR, and GST activities were also quantified in aliquots taken at time 0 and after 2 h of incubation (samples were kept frozen at −80 °C until assay). For determination of intracellular Ca^{2+}, the cardiomyocytes were preloaded with Fluo-3AM (see Flow Cytometric Analysis of Intracellular Ca^{2+}) and sample aliquots were taken every 15 min during 1.5 h of incubation.

Cell Morphology. The severity of cell injury was assessed by microscopic examination of cardiomyocyte morphology in the presence or absence of trypan blue. Approximately 600 cardiomyocytes in each sample aliquot were counted under a light microscope, and the percentage of rod-shaped cells to the total cells was calculated and used as an indicator of the morphological change. Cells with ratio length/width > 3 were classified as rod-shaped cells.

HPLC-DAD Analysis of Aminochromes. α-MeDA, N-Me-α-MeDA, and their respective aminochromes were quantified by HPLC with DAD at 278 (for catecholamines) and 490 nm (for aminochromes), as previously reported (*26*) with slight modifications. Perchloric acid (5% final concentration) was added to aliquots of cell suspension, mixed, and immediately centrifuged for 15 s. The supernatant was neutralized with $KHCO_3$, centrifuged for 15 s, and injected into the HPLC-DAD system. A Waters Spherisorb RP-18 (5 μm) column was used. The mobile phase consisted of 10 mM ammonium acetate and 10% acetonitrile (adjusted to pH 3.0), at a flow rate of 1.0 mL/min. The standard curve of each aminochrome was estimated by total oxidation of known concentrations of α-MeDA or N-Me-α-MeDA with 2 mM $NaIO_4$ in a 50 mM potassium phosphate buffer (pH 7.4). The reactions were conducted at room temperature with vigorous shaking for 2 min. Samples were immediately injected into the HPLC-DAD system. Fractions containing each aminochrome were collected, and the structure was confirmed by mass spectrometry (see Mass Spectrometry of N-Me-α-MeDA and α-MeDA Aminochromes). The total oxidation of α-MeDA or N-Me-α-MeDA into the respective aminochromes was assumed since (i) the peak of α-MeDA or N-Me-α-MeDA in the chromatograms at 278 nm was absent and (ii) the same treatment applied to known concentrations of epinephrine produced similar concentrations of adrenochrome (confirmed by injection of adrenochrome standards).

Mass Spectrometry of N-Me-α-MeDA and α-MeDA Aminochromes. Aminochrome HPLC fractions were collected and analyzed by electrospray mass spectrometry and MS/MS. Electrospray mass spectra and tandem mass spectra were acquired with a Q-TOF 2 (Micromass, Manchester). The instrument resolution was set at 9500 (50% peak valley). The capillary needle voltage was 3000 V, and the source temperature was maintained at 150 °C. Argon was used as the collision gas. The cone voltage was at 45 V for MS and MS/MS. Collision-induced decomposition mass spectra (MS/MS) were acquired by selecting the desired ion with the quadrupole section of the mass spectrometer and colliding it in the collision cell with argon gas (measured pressure in the penning gauge $\sim 6 \times 10^{-6}$ mBar) using a collision energy of 20−25 eV. The resulting product ions were determined by the TOF analyzer. Data acquisition was carried out with a Micromass MassLynx 3.4 data system. Sample introduction used a syringe pump at a flow rate of 10 μL/min.

Biochemical Analysis. The GSH and GSSG contents of cell suspensions were determined by the DTNB−GSSG reductase recycling assay as described before (*16*). Measurement of the adenine nucleotides ATP and ADP in cardiomyocytes was performed by HPLC with UV detection, by a modification of a previously reported method (*27*). Briefly, sample aliquots were treated with perchloric acid (5% final acid concentration) for protein precipitation and centrifuged for 10 min at 13 000 rpm. The supernatant was neutralized with 0.76 M $KHCO_3$, and the sample was centrifuged for 1 min at 13 000 rpm. A volume of 100 μL was then injected into the HPLC system. A Waters Spherisorb RP-18 (5 μm) was the analytical column. The mobile phase consisted of 0.1 M KH_2PO_4, adjusted to pH 6.8. An isocratic elution was performed at 1.0 mL/min at room temperature, and detection was performed at 254 nm. Quantitative measurements were carried out by injection of standard solutions of known concentrations of ATP and ADP. A Compaq computer fitted with Millennium software from Waters processed the chromatographic data.

For the determination of GPX, GR, and GST activity, aliquots of cell suspensions were sonicated for 12 s at medium intensity and then centrifuged at 13 000 rpm for 5 min. The GPX, GR, and GST activities were determined in the supernatant as previously described (*28*).

Flow Cytometric Analysis of Intracellular Ca^{2+}. Real-time intracellular Ca^{2+} measurements were performed only in cardiomyocytes incubated with 1.6 mM N-Me-MeDA. Analysis of intracellular Ca^{2+} was performed as previously reported by Boston et al. (*29*) with some modifications. Ionized calcium was measured using the Ca^{2+} sensitive fluorescent probe, fluo-3 AM, and flow cytometric analysis was performed on a EPICS XL flow cytometer (Beckman-Coulter, Brea, CA) with an argon ion laser (488 nm, 15 mW). Cardiomyocytes (2.5×10^5 cells/mL in modified Krebs−Henseleit buffer) supplemented with 1.8 mM $CaCl_2$ (pH 7.2) were incubated with 10 μM Fluo-3 for 30 min at room temperature. Cells were then washed with fresh Krebs−Henseleit buffer containing 1.8 mM $CaCl_2$, and the cell suspension without treatment (control) was run in a flow cytometer to measure Fluo-3 basal fluorescence (time zero). After that, cells were incubated with 1.6 mM N-Me-MeDA for 90 min at 37 °C in the dark, and samples were taken for analysis every 15 min. To prevent leakage of Fluo-3 via the anion transporter (*30*), probenecid 0.5 mM was added to loading, wash, and protocol solutions.

PI (final concentration 7.5 μM) was added 3 min before data acquisition. PI is an impermeant ion that is fluorescent when bound to DNA and is therefore a marker for nonviable cells. Approximately 10^4 cardiomyocytes in each sample were analyzed for emission fluorescence intensity. Data were collected for emission intensity at wavelengths of 525 nm for Fluo-3 and 675 nm for PI and recorded simultaneously. Only those cells with a low PI fluorescence (viable cells) were included in the comparative analysis of intracellular Ca^{2+}. In these experiments, the Fluo-3 fluorescence intensity was not calibrated; thus,

results are presented as fluorescence arbitrary units and normalized by determining the fluorescence ratio (fluorescence ratio = mean Fluo-3 fluorescence in cells exposed to N-Me-α-MeDA/mean Fluo-3 fluorescence in cells at time zero).

Statistical Analysis. Results are given as means ± SEM (from four to six experiments of different preparations of cardiomyocytes). Statistical comparisons between groups were performed by one way ANOVA followed by Scheffé's test. Changes in the evaluated parameters with time of incubation were evaluated by repeated measures ANOVA (Huynh−Feldt adjustment). When differences reached statistical significance, multiple comparisons between groups were made using the Bonferroni adjustment. Significance was accepted at P less than 0.05.

Results

No toxic effects on cell morphology, intracellular levels of GSH, GSSG, Ca^{2+}, ATP, ADP, or on the activities of GR, GPX, and GST were found after exposure of rat cardiomyocytes to MDMA or MDA at any of the tested concentrations for 4 h (data not shown). In contrast, their catechol metabolites N-Me-α-MeDA and α-MeDA induced significant toxicity in rat cardiomyocytes. One of these effects was an alteration in cell morphology. Figure 2A illustrates normal rod-shaped cardiomyocytes with a regular sarcomere pattern after 2 h of incubation (control group). Isolated cardiac myocytes exposed to N-Me-α-MeDA or α-MeDA underwent a rapid contracture to a square configuration (rigor shortening) (Figure 2B). Contracted cardiomyocytes excluded trypan blue (Figure 2C), indicating that the barrier functions of the plasma membrane were unaffected by rigor shortening. Figure 3A,B shows that both metabolites induced a time- and concentration-dependent loss of rod-shaped morphology that was more evident for N-Me-α-MeDA. Noteworthy, 1.6 mM N-Me-α-MeDA induced more than 90% loss of normal cell morphology after 2 h of incubation. Nevertheless, cellular viability, as measured by trypan blue exclusion, was not significantly different from control cells even after 4 h of incubation (data not shown), although blebs were present in the sarcolemma of cells exposed to N-Me-α-MeDA (0.8−1.6 mM) or α-MeDA (1.6 mM) after 4 h of incubation.

To correlate the toxicological responses at the cellular level with N-Me-α-MeDA and α-MeDA oxidation process, N-Me-α-MeDA, α-MeDA, and their oxidation products (aminochromes) were quantified in cell suspensions incubated with the highest concentration for 4 h. Figure 4A shows N-Me-α-MeDA and N-Me-α-methyldopaminochrome concentrations in cardiomyocyte suspensions exposed to 1.6 mM N-Me-α-MeDA. N-Me-α-MeDA levels decreased from 1.6 mM at time zero to 1.3, 0.8, 0.35, and 0.1 mM after 1, 2, 3, and 4 h of incubation, respectively. The decrease of N-Me-α-MeDA seems to result from its oxidation, as suggested by the appearance of a red coloration in the incubation medium of cell suspensions incubated with 1.6 mM N-Me-α-MeDA after ∼1 h of incubation. In fact, N-Me-α-MeDA aminochrome was detected in cell suspensions after 1 h of incubation, and its concentration increased after 2 h (0.18 and 0.32 mM after 1 and 2 h of incubation, respectively). However, aminochrome levels decreased to 0.22 and 0.14 mM after 3 and 4 h of incubation, respectively. These results are in accordance with the observation that incubation medium of cell suspensions exposed to N-Me-α-MeDA (1.6 mM) became strongly red-colored after ∼2 h of incubation and progressively changed to a dark brown color with the appearance of insoluble black pigments after ∼3 h of incubation. The insoluble black pigments formed are likely to be melanin type (*22*, *23*). Thus, the progressive decreases in N-Me-α-MeDA concentrations, without increase in aminochrome concentrations, and the

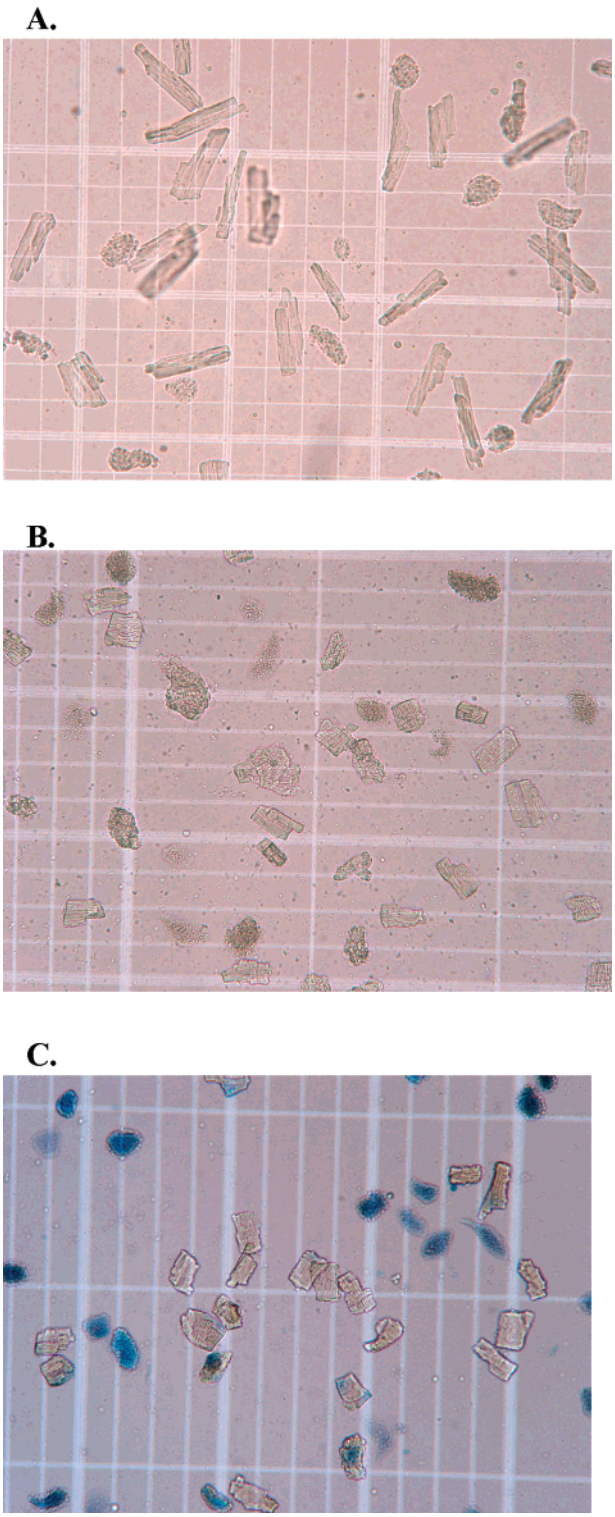

Figure 2. (A) Optic microscopic image of isolated cardiomyocyte suspension showing characteristic rod-shaped cells with a regular sarcomere pattern (control group, 2 h). (B) Cardiomyocytes incubated with N-Me-α-MeDA (1.6 mM, 2 h) underwent a drastic reduction in cell length (rigor shortening). (C) Optic microscopic image showing exclusion of trypan blue dye by contracted cells. Original field magnification, 20×.

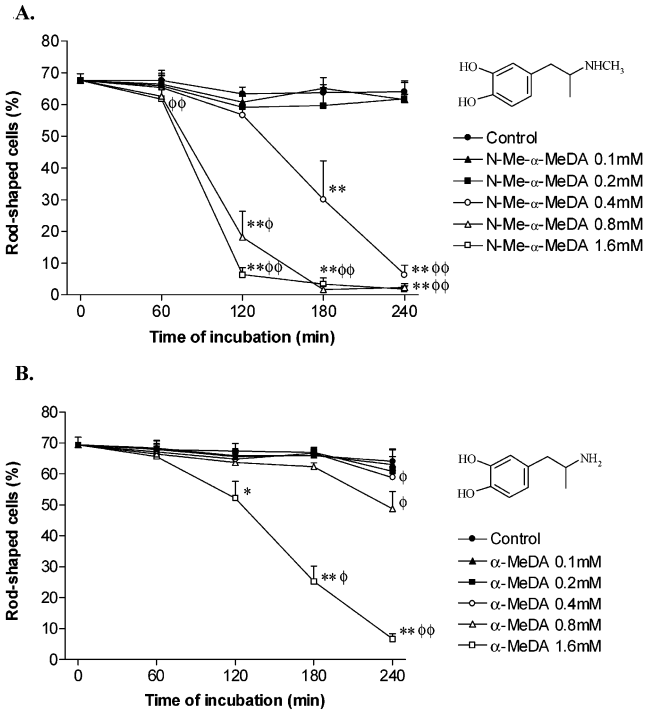

Figure 3. Effect of N-Me-α-MeDA (A) and α-MeDA (B) in cell morphology, measured as % of rod-shaped cells in cardiomyocyte suspensions. Data represent means ± SEM; $n = 5$; $^{*}P < 0.05$ and $^{**}P < 0.01$, as compared with control; $^{\phi}P < 0.05$ and $^{\phi\phi}P < 0.01$, as compared with time zero.

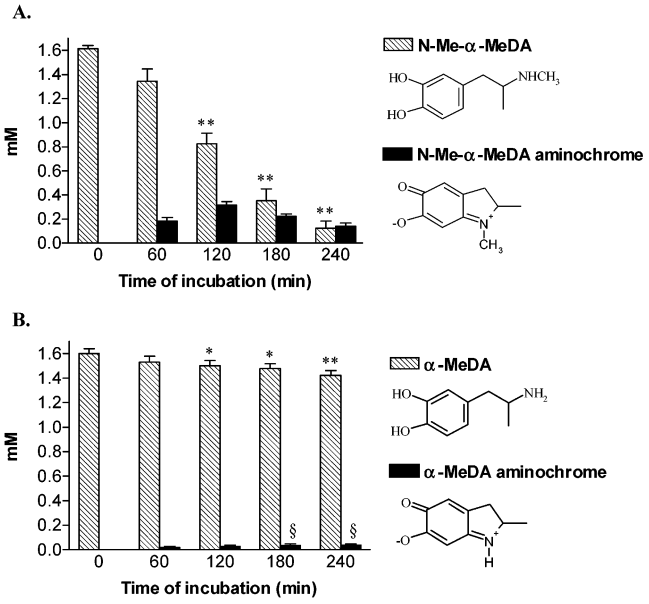

Figure 4. Concentrations of N-Me-α-MeDA and N-methyl-α-methyldopaminochrome (A) and α-MeDA and α-methyldopaminochrome (B) in cardiomyocyte suspensions incubated with 1.6 mM N-Me-α-MeDA or 1.6 mM α-MeDA during 4 h. Data represent means ± SEM; $n = 5$; $^{*}P < 0.05$ and $^{**}P < 0.01$, as compared with control; $^{\S}P < 0.05$, as compared with time 1 h.

appearance of black pigments are suggestive that N-Me-α-MeDA oxidation progresses into formation of melanin type polymers.

In α-MeDA samples, α-MeDA concentrations decreased slightly (but significantly) throughout the incubation period (from 1.6 mM at time zero to 1.53, 1.50, 1.48, and 1.42 mM after 1, 2, 3, and 4 h of incubation, respectively) and this was accompanied by the appearance of an orange coloration in the incubation medium after ∼1 h

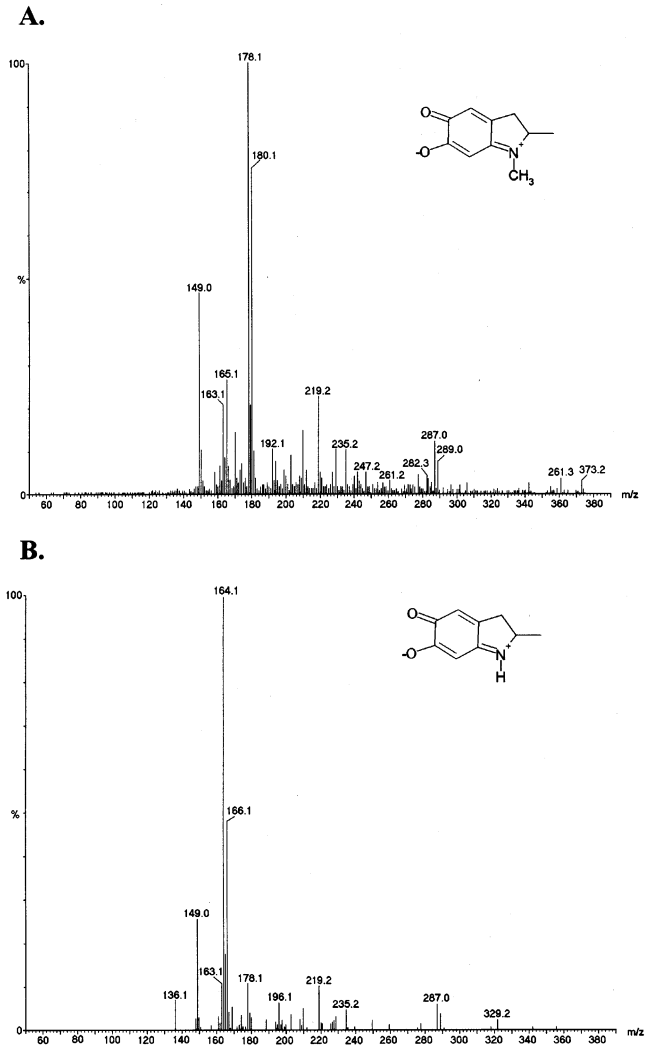

Figure 5. MS spectra of HPLC collected fractions corresponding to N-methyl-α-methyldopaminochrome (A) and to α-methyldopaminochrome (B).

of incubation and of insoluble brown pigments after ∼3−4 h of incubation (Figure 4B). Thus, decreases in α-MeDA concentration were smaller and slower than those observed in N-Me-α-MeDA incubations and accompanied by a smaller formation of the respective aminochrome.

UV spectra of aminochromes presented maximum absorption wavelengths at 220, 305, and 490 nm and were similar to the spectrum of aminochromes obtained after oxidation of N-Me-α-MeDA or α-MeDA with $NaIO_4$ (data not shown). Confirming these results, collected HPLC fractions analyzed by MS showed in their spectra the aminochrome $[M + H]^+$ ion as the base peak, respectively, at *m*/*z* 178.1 for the protonated N-methyl-α-methyldopaminochrome and at *m*/*z* 164.1 for the protonated α-methyldopaminochrome (Figure 5A,B). Additionally, the aminochromes were structurally identified using tandem mass spectrometry, by applying a general fragmentation pattern characteristic of this class of compounds (*31*).

Both N-Me-α-MeDA and α-MeDA induced marked time- and concentration-dependent GSH depletion (Figure 6A,B, respectively), a fact that was already evident for both metabolites after 1 h of incubation. However, GSH depletion was not accompanied by increases in GSSG levels (Figure 7A,B), with the exception of cells exposed to 0.8 mM N-Me-α-MeDA after 1 h of incubation

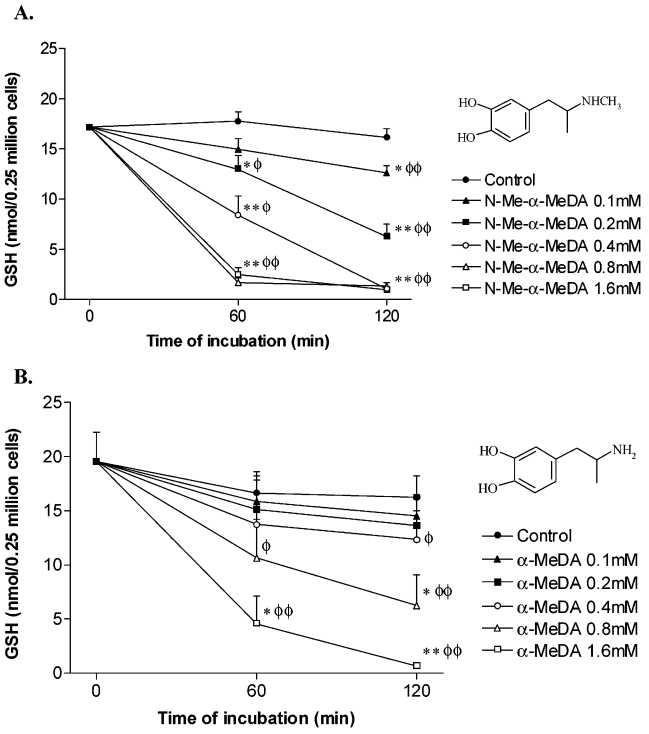

Figure 6. Effect of N-Me-α-MeDA (A) and α-MeDA (B) on GSH levels in cardiomyocyte suspensions. Data represent means ± SEM; $n = 5-6$; $^{*}P < 0.05$ and $^{**}P < 0.01$, as compared with control; $^{\phi}P < 0.05$ and $^{\phi\phi}P < 0.01$, as compared with time zero.

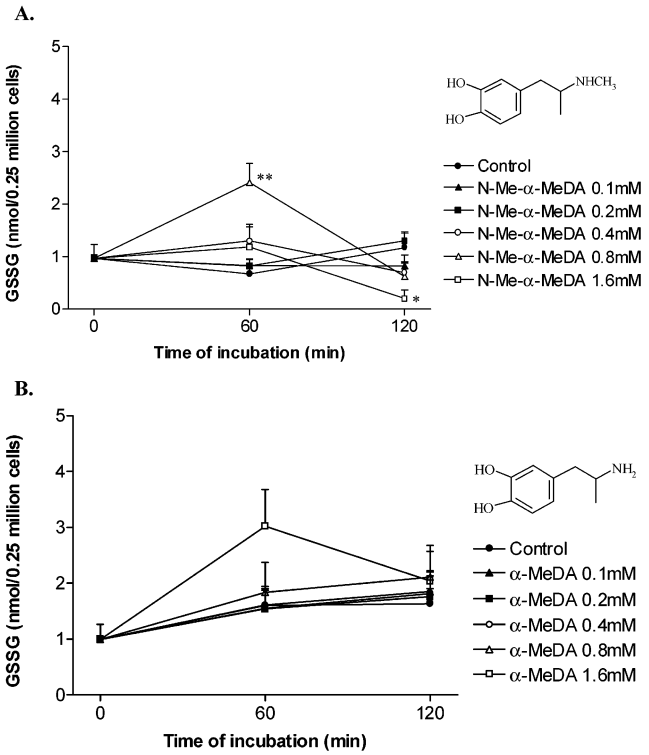

Figure 7. Effect of N-Me-α-MeDA (A) and α-MeDA (B) on GSSG levels in cardiomyocyte suspensions. Data represent means ± SEM; $n = 5-6$; $^{*}P < 0.05$ and $^{**}P < 0.01$, as compared with control.

where a slightly but significant increase in GSSG levels was observed, which seems to indicate a GSH depletion by adduct formation.

A potential effect of N-Me-α-MeDA in cellular Ca^{2+} homeostasis was evaluated by flow cytometry. Figure 8A shows examples of representative results of flow cytometry and dot plots of Fluo-3 and PI fluorescence intensities. The PI negative cells (enclosed in region R) were considered viable cells. Fluorescence intensity of Fluo-3 from viable cells was increased after 45 min of exposure to N-Me-α-MeDA (1.6 mM). The time course of increases in intracellular Ca^{2+} levels in cells exposed to 1.6 mM N-Me-α-MeDA is illustrated in Figure 8B. Disruption of Ca^{2+} homeostasis seems to be an early event since a significant increase in intracellular Ca^{2+} was observed after 45 min of incubation.

The energetic status of the cells was also evaluated. ATP levels were significantly decreased in cell suspensions incubated with N-Me-α-MeDA or α-MeDA (Figure 9A,B, respectively). N-Me-α-MeDA-induced ATP depletion was time- and concentration-dependent and clearly more drastic when compared with α-MeDA. ADP levels were not statistically different when compared with control (data not shown).

Another parameter evaluated, which is important for the cell response to oxidative stress, was the activity of the enzymes GR, GST, and GPX. Figure 10 shows that the activity of these enzymes was significantly lower in samples incubated for 2 h with N-Me-α-MeDA (0.4−1.6 mM) or α-MeDA (1.6 mM) than in control samples.

Discussion

MDA, N-Me-α-MeDA, and α-MeDA are major hepatic-derived metabolites of MDMA (*12*, *32*). These metabolites formed in liver cells may reach the heart through circulation and exert their toxic effects. It may be postulated that if circulating concentrations of the catecholamines N-Me-α-MeDA and α-MeDA become excessive, with a concomitant saturation of catechol-*o*-methyltransferase systems, then enzymatic, cellular, and autoxidative mechanisms (in those cell compartments where their concentration has increased) could lead to the formation of potentially toxic products such as free radical species, *ortho*-quinones, and aminochromes. In the present study, it was found that N-Me-α-MeDA and α-MeDA induced significant toxicity in isolated rat cardiomyocytes; in contrast, MDMA and MDA were not toxic to rat cardiomyocytes, which indicates a lack of MDMA metabolism in this in vitro model, under the experimental conditions used.

Consistent with known pathways of catecholamine oxidation, incubation of rat cardiomyocytes with N-Me-α-MeDA or α-MeDA resulted in the formation of N-methyl-α-methyldopaminochrome and α-methyldopaminochrome, respectively (Figure 4A,B). Higher levels of aminochrome were obtained after incubation with N-Me-α-MeDA when compared to α-MeDA. The presence of a N-methyl group in catecholamines has been reported to increase dramatically the cyclization rate (*33*). Differences in the rate of cyclization of these catechol metabolites may account for the differences observed in their potencies for producing cardiotoxic effects. The aminochrome can also undergo further oxidation. In fact, as the oxidation progressed, a dark brown/black turbidity appeared in the incubation medium, a consequence of melanin type polymer formation (*23*, *34*). It was reported that oxidation of dopamine by enzymatic and nonenzymatic systems gives rise to a black, insoluble polymer only when the concentrations of sulfhydryls such as GSH and cysteine are low relative to that of dopamine (*34*, *35*).

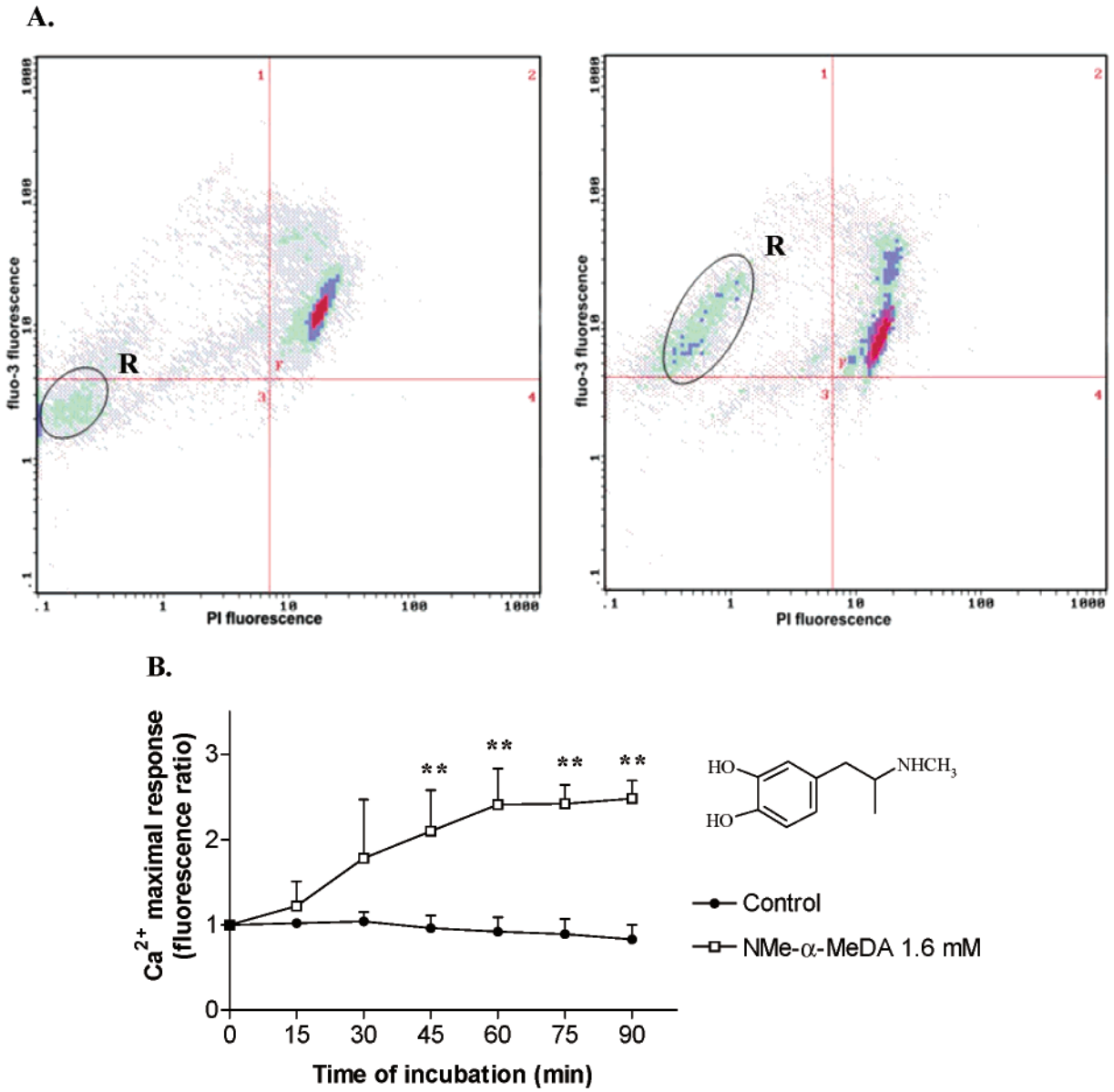

Figure 8. (A) Examples of representative results of flow cytometry. Biparametric dot plots of fluo-3 and PI fluorescence intensities, in control cells (left) and in cells exposed to 1.6 mM N-Me-α-MeDA for 45 min (right). PI negative (viable) cells are gated in region R of the scattergrams. (B) Time course of increase in intracellular Ca^{2+} levels in cells exposed to 1.6 mM N-Me-α-MeDA. Fluorescence ratio = mean Fluo-3 fluorescence in cells exposed to N-Me-α-MeDA/mean Fluo-3 fluorescence in cells at time zero. Data represent means ± SEM; $n = 4$; $^{**}P < 0.01$, as compared with control.

Consistent with these reports, the formation of black pigments in the incubation medium of cells incubated with N-Me-α-MeDA or α-MeDA only occurs as a late stage event. This arises probably from the depleted GSH concentrations (and of the enzymatic antioxidant defense systems) being unable to react with the *ortho*-quinones that were formed within cells (with the result of further oxidation of quinones to melanin type polymers). Melanins represent a large group of chemically active and potentially toxic substances (*36*). Melanins, their intermediates, and reactive oxygen side products exist naturally in vivo and have been implicated in the development of a wide variety of diseases, including cardiovascular disease (for a review see, ref *36*). In the presence of Fe^{3+}, synthetic melanin can catalyze a Fenton type reaction, which generates the hydroxyl radical and initiates lipid peroxidation (*37*). Thus, future work is therefore clearly required to investigate the toxicity exerted by these polymers in cardiomyocytes.

One of the early toxic events observed in cells exposed to N-Me-α-MeDA or α-MeDA was GSH depletion, which was clearly more drastic for the metabolite N-Me-α-MeDA (Figure 6A,B). Oxidation of these catecholamines results in reactive *ortho*-quinones and/or aminochromes, which undergo conjugation with GSH to form the corresponding glutathionyl adducts. Although we did not measure the thiol adduct formation in cardiomyocytes incubated with the catechol metabolites, a drastic depletion on GSH levels was observed without the corresponding enhancement in GSSG levels (Figure 7A,B). It was already shown, in a previous study using freshly isolated rat hepatocytes, that this effect is in fact due to the formation of the GSH conjugates 2-(glutathion-S-yl)-α-MeDA and 5-(glutathion-S-yl)-α-MeDA (*16*). The ability of polyphenolic thioether conjugates to undergo further redox cycling and produce ROS (*12*) provides a rationale for the potential role of these metabolites in MDMA-induced cardiotoxicity. Furthermore, as an endogenous

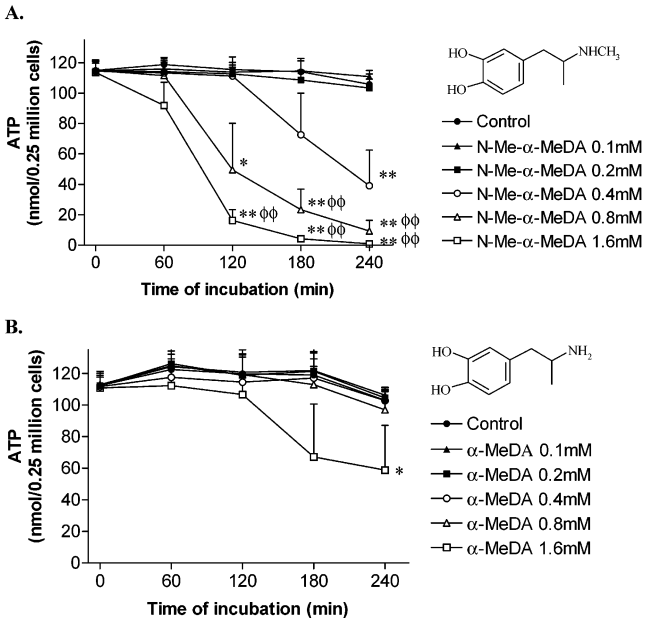

Figure 9. Effect of N-Me-α-MeDA (A) and α-MeDA (B) on ATP levels in cardiomyocyte suspensions. Data represent means ± SEM; $n = 5$; *$P < 0.05$ and **$P < 0.01$, as compared with control; $^{\phi\phi}P < 0.01$, as compared with time zero.

antioxidant, GSH is known to play a crucial protective role against cellular injury, which is due to oxidant neutralizing, lipid peroxidase, and/or tocopheryl-radical regenerating activities (*38*). Thus, GSH depletion may render the cells more exposed to the effects of reactive compounds, ROS, and RNS being formed within the cells, leading to deleterious effects in cardiomyocytes. The ability of N-Me-α-MeDA (0.4−1.6 mM, 2 h) or α-MeDA (1.6 mM, 2 h) to inhibit the activities of GR, GPX, and GST (Figure 10A,B) may be related to either the oxidation or the alkylation of sulfhydryl groups present within the enzyme active site. *ortho*-Quinones, aminochromes, and GSH conjugates are known to cause irreversible inhibition of enzymes that possess either a GSH binding site and/or cysteine residues critical for enzyme function (*23*, *39*, *40*). Inhibition of GR and GST by quinones, as well as GR, GPX, and GST by aminochromes, has been reported (*26*, *41*). GSH in conjunction with GPX/GR is responsible for the elimination of cellular H_2O_2 and organic peroxides. Thus, depletion of GSH and/or decreased activity of these enzymes may compromise this pathway thereby allowing H_2O_2 to accumulate to toxic levels.

The ultimate toxic event observed in cells exposed to N-Me-α-MeDA or α-MeDA was the onset of rigor shortening resulting in loss of rod-shaped morphology (Figures 2 and 3), which is an index of cardiomyocyte injury. Importantly, cell contracture occurred without loss of sarcolemmal integrity, which indicates that this injury is clearly distinct from the common measure of cell death defined by trypan blue exclusion or other sarcolemma permeability changes. Hypercontracture of isolated myocytes may correspond to the formation of contraction bands in hearts of individuals who died after using MDMA (*2*). There are some mechanisms that may be responsible for cell contracture, namely, intracellular Ca^{2+} overload as well as GSH or ATP depletion. A complex link exists between intracellular thiol status and Ca^{2+} homeostasis. Indeed, oxidation of sulfhydryl groups of membrane-associated proteins in either mitochondria and/or other intracellular compartments may lead to a disruption of ion homeostasis, especially Ca^{2+} (*42*).

Regulation of intracellular Ca^{2+} is essential for normal function of the myocardium, and alterations of Ca^{2+} homeostasis have been linked to the development of pathological conditions, such as arrhythmias (*43*). In this study, N-Me-α-MeDA-induced rigor shortening occurs without loss of sarcolemmal integrity. Cell contracture, therefore, is not secondary to a massive loss of ATP and gain in Ca^{2+} following breakdown of the sarcolemmal barrier. This suggests that increases in cytosolic Ca^{2+} levels may result from Ca^{2+} release from intracellular

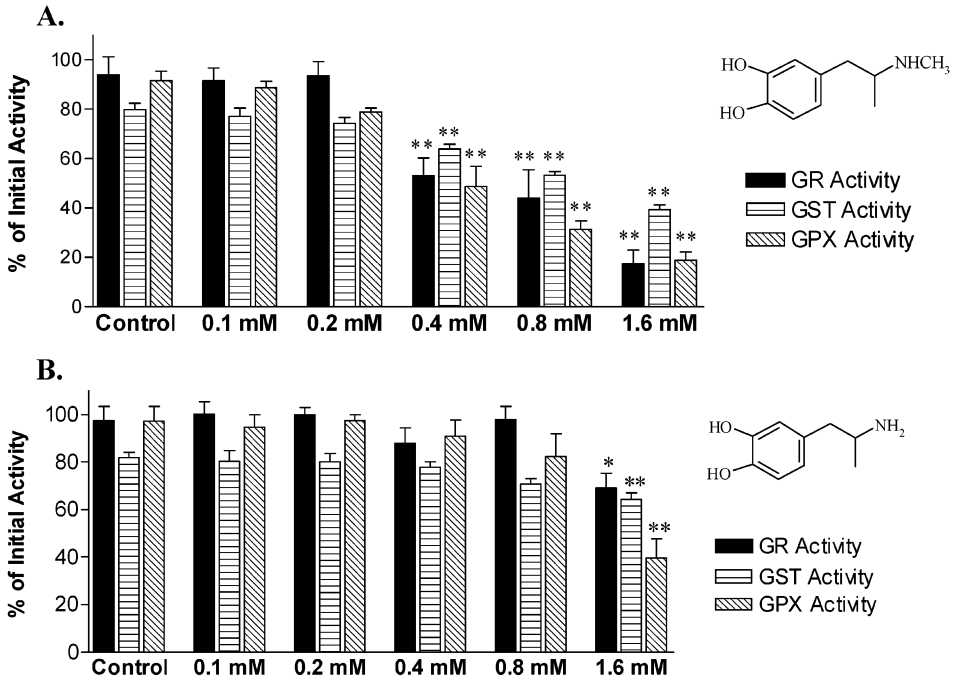

Figure 10. Percentage of GR, GST, and GPX activities after 2 h of N-Me-α-MeDA (A) or α-MeDA (B) incubation in cardiomyocyte suspensions relative to initial activities. Data represent means ± SEM; $n = 6$; *$P < 0.05$ and **$P < 0.01$, as compared with control.

stores, namely, mitochondria and sarcoplasmic reticulum. Indeed, quinones are known to cause disruption of intracellular Ca^{2+} homeostasis by release of Ca^{2+} from intracellular stores (mitochondria and endoplasmatic reticulum) and inhibition of Ca^{2+} efflux from the cell (*44*). Additionally, aminochromes have been reported to inhibit the mitochondrial and sarcoplasmic reticular Ca^{2+} uptake system (*23*).

The onset of contracture in cells exposed to N-Me-α-MeDA or α-MeDA (Figure 3A,B) could be also correlated with decreases in intracellular ATP levels (Figure 9A,B). Aminochromes have been reported to affect mitochondrial energy processes (*23*, *45*). Our results suggest that N-Me-α-MeDA, α-MeDA, or their oxidation products in the myocardial cell may impair the process of energy production in mitochondria (which unable cell myofibrils to return to the resting state). The overall process may result in contractile failure of hearts exposed to these cardiotoxic metabolites of MDMA.

It is worthwhile to refer that in this study a drastic depletion of GSH and ATP levels were observed without loss of sarcolemma integrity. Thus, it appears that the observed depletion of nonprotein thiols, such as GSH, or ATP depletion are not sufficient per se to induce death of cardiac myocytes. In agreement, previous reports of Timerman et al. (*42*) showed that total GSH could be depleted from 11 to 1 nmol/mg protein without affecting the integrity of the sarcolemmal barrier. Also, adult myocytes depleted of even 70% of their ATP were reported to retain essentially normal rod-shaped morphology (*46*). Given the predominant role of mitochondria in cardiac muscle metabolism, mitochondrial dysfunction may be particularly important to mechanisms of cell death in cardiomyocytes. It was already shown that peroxidative damage originating in the mitochondria is a major event in the onset of cell death in cardiomyocytes depleted of GSH (*47*). Thus, our results seem to indicate that cell death provoked by N-Me-α-MeDA or α-MeDA would occur as a late stage event, which probably will be due to the depletion of mitochondrial GSH. Mitochondria would then be unable to detoxify H_2O_2 and organic peroxides being formed within this organelle; this may result in membrane peroxidative damage and initiation of a cascade of events leading to necrosis or apoptosis, depending on several factors, namely, the putative efflux of mitochondrial apoptotic factors and cellular energy status.

The concentrations of MDMA metabolites used in the present study may be considered above those found in human abusers, usually in the low micromolar range (*48*). However, the evaluation of acute toxicity of MDMA and/or its metabolites as is the case of the present study (this type of study with freshly isolated cardiomyocytes is only reliable in incubations up to 4 h since the biochemical characteristics of the cells tend to be lost after this time) needs to address higher concentrations than those usually obtained during chronic use of this drug. In fact, it is important to evaluate the mechanistic interactions of MDMA and/or its metabolites with cellular components, which is only possible at the concentrations used. A lower but longer effect during in vivo chronic exposure may also be exceptionally deleterious to the heart, although further studies are needed to confirm this hypothesis. Importantly, tissue concentrations of MDMA and its metabolites have been reported to be substantially higher (up to 18 times) than blood concentrations (*48*, *49*). Thus, new studies are also needed to verify which heart concentrations are achieved for MDMA and its toxic metabolites during intoxications with this drug of abuse. Notably, it was already reported that in humans, N-Me-α-MeDA, a major toxic metabolite in the present study, reaches plasma concentrations similar to those of MDMA (*50*).

In conclusion, the present findings show that MDMA metabolites, N-Me-α-MeDA and α-MeDA, but not the parent compound, induce significant toxicity to freshly isolated rat cardiomyocytes, N-Me-α-MeDA being the most toxic of the metabolites studied. The loss of GSH and the modification of enzyme activities induced by N-Me-α-MeDA, α-MeDA, and/or their oxidation products, clearly show that one of the early consequences of MDMA metabolism is a disruption of thiol homeostasis, which may result in disruption of Ca^{2+} homeostasis, ATP depletion, and cell contracture. Thus, metabolism of MDMA, resulting in the formation of the highly reactive compounds N-Me-α-MeDA and α-MeDA, is required for the expression of MDMA-induced cardiotoxicity in vitro.

Acknowledgment. This work was supported by Ph.D. grants from FCT (Praxis XXI/BD/20087/99 and Praxis XXI/BD/18520/98) and POCTI, Portugal, and by FEDER European Community funding (Project POCTI/36099/FCB/2000).

References

(1) Henry, J. A., Jeffreys, K. J., and Dawling, S. (1992) Toxicity and deaths from 3,4-methylenedioxymethamphetamine ("ecstasy"). *Lancet 340*, 384−387.

(2) Milroy, C. M., Clark, J. C., and Forrest, A. R. W. (1996) Pathology of deaths associated with "ecstasy" and "eve" misuse. *J. Clin. Pathol. 49*, 149−153.

(3) Suarez, R., and Riemersma, R. (1988) "Ecstasy" and sudden cardiac death. *Am. J. Forensic Med. Pathol. 9*, 339−341.

(4) O'Cain, P., Hletko, S., Ogden, B., and Varner, K. (2000) Cardiovascular and sympathetic responses and reflex changes elicited by MDMA. *Physiol. Behav. 70*, 141−148.

(5) Lester, S. J., Baggott, M., Welm, S., Schiller, N. B., Jones, R. T., Foster, E., and Mendelson, J. (2000) Cardiovascular effects of 3,4-methylenedioxymethamphetamine. A double-blind, placebo-controlled trial. *Ann. Intern. Med. 133*, 969−973.

(6) Fitzgerald, J. L., and Reid, J. J. (1994) Sympathomimetic actions of methylenedioxymethamphetamine in rat and rabbit isolated cardiovascular tissues. *J. Pharm. Pharmacol. 46*, 826−832.

(7) Varner, K. Y., Delcarpio, J. B., and Moerschbaecher, J. M. (1998) Cardiac toxicity elicited by repeated administration of 3,4-methylenedioxymethamphetamine (MDMA). *NIDA Res. Monogr. 179*, 214.

(8) Rona, G. (1985) Catecholamine cardiotoxicity. *J. Mol. Cell Cardiol. 17*, 291−306.

(9) Wheatley, A. M., Thandroyen, F. T., and Opie, L. H. (1985) Catecholamine-induced myocardial cell damage: catecholamines or adrenochrome? *J. Mol. Cell Cardiol. 17*, 349−359.

(10) Gesi, M., Lenzi, P., Soldani, P., Ferrucci, M., Giusiani, A., Fornai, F., and Paparelli, A. (2002) Morphological effects in the mouse myocardium after methylenedioxymethamphetamine administration combined with loud noise exposure. *Anat. Rec. 267*, 37−46.

(11) He, S. Y. (1995) Methamphetamine-induced toxicity in cultured adult rat cardiomyocytes. *Nippon Hoigaku Zasshi 49*, 175−186.

(12) Bai, F., Lau, S. S., and Monks, T. J. (1999) Glutathione and *N*-acetylcysteine conjugates of α-Methyldopamine produce serotoninergic neurotoxicity: possible role in methylenedioxyamphetamine-mediated neurotoxicity. *Chem. Res. Toxicol. 12*, 1150−1157.

(13) Bai, F., Jones, D. C., Lau, S. S., and Monks, T. J. (2001) Serotonergic Neurotoxicity of 3,4-(±)-Methylenedioxyamphetamine and 3,4-(±)-Methylenedioxymethamphetamine (Ecstasy) Is Potentiated by Inhibition of gamma-Glutamyl Transpeptidase. *Chem. Res. Toxicol. 14*, 863−870.

(14) Miller, R. T., Lau, S. S., and Monks, T. J. (1996) Effects of intracerebroventricular administration of 5-(glutathion-S-yl)-α-Methyldopamine on brain dopamine, serotonin, and norepinephrine concentrations in male sprague-dawley rats. *Chem. Res. Toxicol. 9*, 457−465.

(15) Miller, R. T., Lau, S. S., and Monks, T. J. (1997) 2,5-bis-(Glutathion-S-yl)-α-Methyldopamine, a putative metabolite of (±)-3,4-methylenedioxyamphetamine, decreases brain serotonin concentrations. *Eur. J. Pharmacol. 323*, 173−180.

(16) Carvalho, M., Milhazes, N., Remião, F., Borges, F., Fernandes, E., Monks, T., Amado, F., Carvalho, F., and Bastos, M. L. (2004) Hepatotoxicity of 3,4-methylenedioxyamphetamine and α-Methyldopamine in isolated rat hepatocytes: formation of glutathione conjugates. *Arch. Toxicol. 78*, 16−24.

(17) Carvalho, M., Hawksworth, G., Milhazes, N., Borges, F., Monks, T., Fernandes, E., Carvalho, F., and Bastos, M. L. (2002) Role of metabolites in MDMA (ecstasy)-induced nephrotoxicity: an in vitro study using rat and human renal proximal tubular cells. *Arch. Toxicol. 76*, 581−588.

(18) Lim, H. K., and Foltz, R. L. (1988) In vivo and in vitro metabolism of 3,4-(methylenedioxy)methamphetamine in the rat: identification of metabolites using an ion trap detector. *Chem. Res. Toxicol. 1*, 370−378.

(19) Kumagai, Y., Lin, L. Y., Schmitz, D. A., and Cho, A. K. (1991) Hydroxyl radical mediated demethylenation of (methylenedioxy)-phenyl compounds. *Chem. Res. Toxicol. 4*, 330−334.

(20) Marquardt, G. M., DiStefano, V., and Ling, L. L. (1978) Metabolism of beta-3,4-methylenedioxyamphetamine in the rat. *Biochem. Pharmacol. 27*, 1503−1505.

(21) Bolton, J. L., Trush, M. A., Penning, T. M., Dryhurst, G., and Monks, T. J. (2000) Role of quinones in toxicology. *Chem. Res. Toxicol. 13*, 135−160.

(22) Bindoli, A., Rigobello, M. P., and Galzigna, L. (1989) Toxicity of aminochromes. *Toxicol. Lett. 48*, 3−20.

(23) Bindoli, A., Rigobello, M. P., and Deeble, D. J. (1992) Biochemical and toxicological properties of the oxidation products of catecholamines. *Free Radical Biol. Med. 13*, 391−405.

(24) Hiramatsu, M., Kumagai, Y., Unger, S. E., and Cho, A. K. (1990) Metabolism of methylenedioxymethamphetamine: formation of dihydroxymethamphetamine and a quinone identified as its glutathione adduct. *J. Pharmacol. Exp. Ther. 254*, 521−527.

(25) Remião, F., Carmo, H., Carvalho, F., and Bastos, M. L. (2001) Cardiotoxicity studies using freshly isolated calcium-tolerant cardiomyocytes from adult rat. *In Vitro Cell Dev. Biol. Anim. 37*, 1−4.

(26) Remião, F., Carvalho, M., Carmo, H., Carvalho, F. D., and Bastos, M. L. (2002) Cu2+-induced isoproterenol oxidation into isoprenochrome in adult rat calcium-tolerant cardiomyocytes. *Chem. Res. Toxicol. 15*, 861−869.

(27) Stocchi, V., Cucchiarini, L., Magnani, M., Chiarantini, L., Palma, P., and Crescentini, G. (1985) Simultaneous extraction and reverse-phase high-performance liquid chromatographic determination of adenine and pyridine nucleotides in human red blood cells. *Anal. Biochem. 146*, 118−124.

(28) Carvalho, M., Carvalho, F., Remião, F., Pereira, M. L., Pires-das-Neves, R., and Bastos, M. L. (2002) Effect of 3,4-methylenedioxymethamphetamine ("ecstasy") on body temperature and liver antioxidant status in mice: influence of ambient temperature. *Arch. Toxicol. 76*, 166−172.

(29) Boston, D., Koyama, T., Rodriguez-Larrain, J., Zou, A., Su, Z., and Barry, W. (1998) Effects of angiotensin II on intracellular calcium and contracture in metabolically inhibited cardiomyocytes. *J. Pharmacol. Exp. Ther. 285*, 716−723.

(30) DiVirgilio, F., Steinberg, T. H., and Silverstein, S. C. (1990) Inhibition of Fura-2 sequestration and secretion with organic anion transport blockers. *Cell Calcium 11*, 57−62.

(31) Lemos-Amado, F., Domingues, P., Ferrer-Correia, A., Remião, F., Milhazes, N., Borges, F., Carvalho, F. D., and Bastos, M. L. (2001) Electrospray tandem mass spectrometry of aminochromes. *Rapid Commun. Mass Spectrom. 15*, 2466−2471.

(32) Kreth, K.-P., Kovar, K.-A., Schwab, M., and Zanger, U. M. (2000) Identification of the human cytochromes P450 involved in the oxidative metabolism of "ecstasy"-related designer drugs. *Biochem. Pharmacol. 59*, 1563−1571.

(33) Chavdarian, C. G., Karashima, D., Castagnoli, N. J., and Hundley, H. K. (1978) Oxidative and cardiovascular studies on natural and synthetic catecholamines. *J. Med. Chem. 21*, 548−554.

(34) Zhang, F., and Dryhurst, G. (1994) Effects of L-cysteine on the oxidation chemistry of dopamine: new reaction pathways of potential relevance to idiopathic Parkinson's disease. *J. Med. Chem. 37*, 1084−1098.

(35) Carstam, R., Brinck, C., Hindemith-Augustsson, A., Rorsman, H., and Rosengren, E. (1991) The neuromelanin of the human substancia nigra. *Biochim. Biophys. Acta 1097*, 152−160.

(36) Hegedus, Z. L. (2000) The probable involvement of soluble and deposited melanins, their intermediates and the reactive oxygen side-products in human diseases and aging. *Toxicology 145*, 85−101.

(37) Ben-Shachar, D., Riederer, P., and Youdim, M. B. (1991) Iron-melanin interaction and lipid peroxidation: implications for Parkinson's disease. *J. Neurochem. 57*, 1609−1614.

(38) DiMascio, P., Murphy, M. E., and Sies, H. (1991) Antioxidant defense systems: the role of carotenoids, tocopherols, and thiols. *Am. J. Clin. Nutr. 53*, 194S−200S.

(39) Ommen, B. V., Ploemen, J. H. T. M., Bogaards, J. J. P., Monks, T. J., Lau, S. S., and Bladeren, P. J. V. (1991) Irreversible inhibition of rat glutathione S-transferase 1-1 by quinones and their glutathione conjugates. Structure−activity relationship and mechanism. *Biochem. J. 276*, 661−666.

(40) Monks, T. J., and Lau, S. S. (1992) Toxicology of quinone-thioethers. *Crit. Rev. Toxicol. 22*, 243−270.

(41) Remião, F., Carmo, H., Carvalho, F. D., and Bastos, M. L. (1999) Inhibition of glutathione reductase by isoproterenol oxidation products. *J. Enzyme Inhib. 15*, 47−61.

(42) Timerman, A. P., Altschuld, R. A., Hohl, C. M., Brierley, G. P., and Merola, A. J. (1990) Cellular glutathione and the response of adult rat heart myocytes to oxidant stress. *J. Mol. Cell Cardiol. 22*, 565−575.

(43) Kang, Y. J. (2001) Molecular and cellular mechanisms of cardiotoxicity. *Environ. Health Perspect. 109*, 27−34.

(44) Orrenius, S., McConkey, D. J., Bellomo, G., and Nicotera, P. (1989) Role of Ca2+ in toxic cell killing. *TIPS 10*, 281−285.

(45) Taam, G. M., Takeo, S., Ziegelhoffer, A., Singal, P. K., Beamish, R. E., and Dhalla, N. S. (1986) Effect of adrenochrome on adenine nucleotides and mitochondrial oxidative phosphorylation in rat heart. *Can. J. Cardiol. 2*, 88−93.

(46) Haworth, R. (1990) Use of isolated adult myocytes to evaluate cardiotoxicity. II. Preparation and properties. *Toxicol. Pathol. 18*, 521−530.

(47) Dhanbhoora, C. M., and Babson, J. R. (1992) Thiol depletion induces lethal cell injury in cultured cardiomiocytes. *Arch. Biochem. Biophys. 293*, 130−139.

(48) Garcia-Repetto, R., Moreno, E., Soriano, T., Jurado, C., Gimenez, M. P., and Menendez, M. (2003) Tissue concentrations of MDMA and its metabolite MDA in three fatal cases of overdose. *Forensic Sci. Int. 135*, 110−114.

(49) Sticht, G., Pluisch, F., Bierhoff, E., and Kaferstein, H. (2003) Fatal outcome of Ecstasy overdose. *Arch. Kriminol. 211*, 73−80.

(50) Segura, M., Ortuno, J., Farre, M., McLure, J. A., Pujadas, M., Pizarro, N., Llebaria, A., Joglar, J., Roset, P. N., Segura, J., and Torre, R. d. L. (2001) 3,4-Dihydroxymethamphetamine (HHMA). A major in vivo 3,4-methylenedioxymethamphetamine (MDMA) metabolite in humans. *Chem. Res. Toxicol. 14*, 1203−1208.

TX049960F